Electrochemical Treatment of C.I. Reactive Black 5 Solutions on Stabilized Doped Ti/SnO$_2$ Electrodes

A.I. del Río, M.J. Benimeli, J. Molina, J. Bonastre, F. Cases[*]

Departamento de Ingeniería Textil y Papelera, Escuela Politécnica Superior de Alcoy, Universitat Politècnica de València. Plaza Ferrándiz y Carbonell, s/n, 03801, Alcoy, Spain.
[*]E-mail: fjcases@txp.upv.es

The electrochemical treatment of wastewaters from the textile industry is a promising technique for substances which are resistant to biodegradation. This paper deals with the electrochemical decolourisation and degradation of synthetic solutions containing a bifunctional reactive dye with a high molecular complexity: C.I. Reactive Black 5. The electrolysis was carried out under galvanostatic conditions employing a filter press reactor with two different configurations. A divided filter press reactor (D-FPR) to study only the oxidation process and an undivided filter press reactor (UD-FPR) to study the oxido-reduction process. All the processes were evaluated using Ti/SnO$_2$–Sb–Pt and stainless steel electrodes as anode and cathode, respectively. The decolourisation and degradation of the dye were tracked by means of total organic carbon (TOC), chemical oxygen demand (COD) measurements, UV-Visible spectroscopy, as well as high performance liquid chromatography (HPLC). The kinetics of decolourisation was of pseudo-first order for both processes. Average Oxidation State (AOS), Carbon Oxidation State (COS) and Average Current Efficiency (ACE) were also determined.

1. INTRODUCTION

Textile wastewaters present highly varying compositions depending on the textile produced. In order to cover both the industrial and environmental necessities, dyes are being continually upgraded and replaced by superior compounds. Therefore, to comply with the current regulations on this matter, one of the objectives of the industry is to obtain textile effluents containing low concentrations of dye [1, 2]. However, even minor concentrations of dyes may have a significant environmental impact [3]. In addition to this, many dyes are toxic and/or mutagenic to aquatic life [4] and, due to the large degree of aromatic rings present in the dye molecules and the stability of modern dyes, biological treatment is ineffective for their degradation [5, 6]. Moreover, as the number of sulphonic groups increases, the

solubility of the dye in water also increases which makes their removal very difficult. The particular case of reactive dyes is of special interest because they undergo, to a certain extent, a hydrolysis reaction. Thus, the hydrolysed dye is no longer capable of reacting with the fibre and so must be washed out of the fibre after the dyeing process is completed. For this reason, the hydrolysed dye and any unreacted dye inevitably end up in the dyehouse effluent. Recently, these problems have been partially reduced with the development of more selective fibre-reactive systems, such as bifunctional reactive dyes, showing significantly improved processing conditions [7, 8]. However, a practical reactive dye system which is completely free of the problem of hydrolysis has not been found yet. An alternative approach to addressing the problem of colour and toxicity in textile dyeing effluent involves the development of effluent treatment methods such as ozonation [9], advanced oxidation processes [10-13], enzymatic [14] or adsorption processes [15] for the removal of different dyes. Over the past 10 years, electrochemical techniques have been found that are of special interest for textile wastewater remediation due to advantages such as high efficiency, ease of operation and environmental compatibility, since there is no need to add chemicals [2]. In light of the above, several researchers have focused on the destruction of these synthetic wastes using electrochemical oxidation [16-22], although electrochemical reduction has been also found to be an interesting method for decolourisation of textile wastewaters [23-27]. In an attempt to evaluate the optimum operational parameters, numerous papers have been published related to the characterisation of several electrode materials. However, DSA electrodes constitute by far one of the most attractive materials for electrochemical treatment.

The present research is aimed at studying the electrochemical treatment of a C.I. Reactive Black 5 solution using two different configurations of a filter press reactor: a divided filter press reactor (D-FPR) and an undivided filter press reactor (UD-FPR). This dye was chosen as a representative dye to explore the suitability of the electrochemical treatment on Ti/SnO_2-Sb-Pt anodes for the efficient removal of reactive azo dyes in aqueous solutions. This kind of electrode combine three important aspects: they present high chemical and electrochemical stability as a consequence of the rather large band gap (roughly 3.5 eV), high electrical conductivity of doped SnO_2 and, finally, these electrodes show high oxygen evolution overpotential (η_{O2}). In order to increase the service life of Ti/SnO_2-Sb electrodes it has been demonstrated that the introduction of small amounts of platinum in the coating produces an increase of the service life of several orders of magnitude. The primary objective in this work is to evaluate the influence of operational parameters such as current density and the type of electrolyte employed on TOC and COD elimination as well as the efficiency of the processes on the decolourisation and degradation of C.I. Reactive Black 5, a Remazol vinylsulphone dye whose molecular weight is 991.8 g mol^{-1}. This dye is intermediate in reactivity between the high-reactivity heterocyclic systems, such as dichlorotriazine (Procion MX type), and the low-reactivity ranges, such as aminochlorotriazine (Procion H), and its molecular complexity is greater than that of other dyes already studied such as Acid Orange 7 [20], Orange II [21], Acid Orange 10 [22], Alizarin Red [28] or C.I. Reactive Orange 16 [29], among others. The molecular structure of C.I. Reactive Black 5 is illustrated in Figure 1, where the main functional groups of the molecule, reactive groups and chromophore groups, are marked.

Figure 1. Molecular structure of C.I. Reactive Black 5.

C.I. Reactive Black 5 was selected as a model compound due to the incomplete fixation reaction on cellulose. The reason is the competition between the reaction of the reactive vinylsulphone groups with the fibre and the reaction of hydrolysis of the vinylsulphone groups giving the 2-hydroxyethylsulphone groups. The 2-hydroxyethylsulphone groups do not react with the fibres which means that the efficiency of the dyeing process diminishes [8, 30].

2. EXPERIMENTAL

2.1. Chemicals

Ultrapure water from an Elix 3 Millipore-Milli-Q Advantage A10 system with a resistivity near to 18.2 MΩ cm was used for the preparation of all solutions. Solutions of C.I. Reactive Black 5 were simulated from the commercial product (provided by Dystar) according to real concentrations found in textile effluents. In fact, textile effluents concentrations vary from 0.01 to 0.25 g L^{-1}, although concentrations about 1 g L^{-1} have also been found [31]. A concentration of 1.0 g L^{-1} was selected as the initial concentration of dye solutions for this work.

Taking into account that the hydrolysed form of reactive dyes is responsible for colour in effluents containing wastewaters from the textile industry, all synthetic dye solutions were previously hydrolysed by the addition of a NaOH solution. As a result of this process, all dye solutions presented an alkaline pH (about 10-13). Moreover, either 0.1 M Na$_2$SO$_4$ or 0.1 M NaCl were the two electrolytes employed in this work (always separately). NaOH and Na$_2$SO$_4$ were supplied by Merck (proanalysis quality). NaCl was provided by Fluka,

2.2. Electrolysis

The electrolysis of the alkaline aqueous solutions containing the hydrolysed dye was carried out using two different configurations. On the one hand, a divided filter press reactor (D-FPR) was considered only to study the oxidation process. This process takes place in the anodic compartment (Figure 2-a) which is separated from the cathodic compartment (where the reduction process occurs) by means of a cationic membrane (Nafion 117, DuPont). This configuration allowed us to carry out the

study of the oxidation process without any interference given by the concurrent reduction of the dye and/or intermediates.
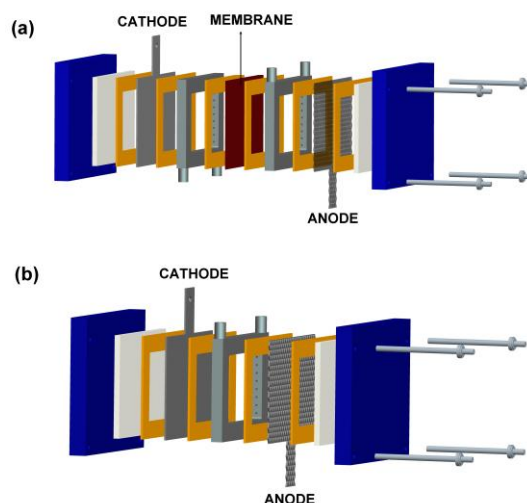

Figure 2. Scheme of the different configurations of the filter press reactor employed in this work: (a) divided filter press reactor (D-FPR); (b) undivided filter press reactor (UD-FPR).

On the other hand, the simultaneous oxidation and reduction process was performed in an undivided filter press reactor (UD-FPR), as it can be seen in Figure 2-b. In this case, no separation between anodic and cathodic compartments was done. This makes feasible the study of both the oxidation and the reduction processes of dye and/or intermediates. Then, the possibility of a synergetic effect between oxidation and reduction processes can be evaluated

A stainless steel electrode was employed as cathode and Ti/SnO$_2$-Sb-Pt electrode with mesh geometry was used as anode. The volume of the dye solution treated was 0.45 L in every case. All the experiments were carried out under galvanostatic conditions with a power supply (Grelco GVD310 0-30Vcc / 0-10 A). The applied current density was 50 and 125 mA cm^{-2} up to a total applied specific charge of 240 Ah L^{-1} (Q_{final}). The final samples could then be compared when the variation of analytical parameters such as TOC and COD was insignificant under the same experimental conditions. Different samples were collected during the experiments but only three different samples were basically considered in all cases. The first was the initial sample (untreated dye solution). The second was the moment of complete decolourisation. This is when the unbroken azo group in solution was only 1 % (determined by means of chromatographic and spectrophotometric measurements). The third was the final sample and was always taken at Q_{final} = 240 Ah L^{-1} [32].

2.3. Preparation of the doped SnO$_2$ electrodes

The electrodes of doped tin dioxide were prepared following a standard thermal decomposition method of salt precursors on a titanium substrate [33-36]. Titanium electrodes with mesh geometry and

48 cm^2 of geometrical area were first pre-treated in order to eliminate the superficial layer of TiO$_2$ (an electric semiconductor). Moreover, a higher roughness was obtained. Thus, the electrocatalytic oxide deposit could be adhered to the support. This pre-treatment consisted of degreasing with acetone using ultrasounds for 10 min. Following this, the titanium supports were etched for 1 h in a boiling solution of oxalic acid (10%). After that, the supports were rinsed with ultrapure water and the precursor solution was brushed onto the Ti mesh. This precursor solution contained 10% SnCl$_4$·5H$_2$O (provided by Aldrich), 1% SbCl$_3$ (purchased from Fluka) for samples containing antimony, and 0.252% H$_2$PtCl$_6$·6H$_2$O (supplied by Merck) for samples containing Pt. All of them were dissolved in a mixture of ethanol (provided by Panreac) + HCl (supplied by Merck). Afterwards, the electrodes were placed in an oven at 673 K for 10 min. In this phase of the procedure, the decomposition of the salt and the formation of the metal oxide takes place. This process was repeated until a weight increment of about 2 mg cm^{-2} was reached. Finally, a thermal treatment at 873 K was applied for 1 h.

2.4. Analyses and instruments

TOC measurements were performed using a Shimadzu TOC-VCSN analyser based on the combustion-infrared method. Samples were diluted to bring their concentration within the operating range of the apparatus. The instrument operated at 1193 K and 20 µL sample injection with an air (free of CO$_2$) flow rate of 150 mL min^{-1}. COD measurements were also done with a Spectroquant analyser.

The method employed for these measurements is analogous to EPA 410.4, US Standard Methods 5220 D and ISO 15705. It is important that the concentration of chloride does not exceed a limit of 2000 mg L^{-1} in order to avoid interference in COD results. For this reason, samples containing chloride in solution had to be diluted. UV-Visible spectra of C.I. Reactive Black 5 solutions and chromatographic analyses were performed using a Hitachi Lachrom-Elite Chromatographic System equipped with diode array detector. The chromatographic separations were performed on a Lichrospher 100 RP-18 C column with 5 µm packing using a method based on the one described in the European regulation EN 14362-2:2003/A where the procedure for the detection of certain azoic dyes is described. Taking this regulation into account, the percentages of the mobile phase composition were adapted to carry out the study presented in this paper. The mobile phase was methanol (eluent A)/aqueous buffer solution KH$_2$PO$_4$·Na$_2$HPO$_4$ (eluent B) with pH 6.9. Separation was accomplished at a flow rate of 1 mL min^{-1}, at 25 ºC and injection volume of 80 µL. The detection wavelength was set at 600 and 250 nm. At the beginning of the chromatographic separations, the gradient elution consisted of 100 % aqueous buffer and it was progressively modified to 100% methanol over 20 min.

3. RESULTS AND DISCUSSION

3.1. TOC and COD removal

Table 1 shows the effect of applied current density and electrolyte on COD and TOC removal percentages. The variations in these parameters were compared as a measure of the ability of the

Ti/SnO$_2$-Sb-Pt electrode to decompose both the starting organic material and the intermediates after 240 Ah L^{-1} of applied specific charge using the filter press reactor.

On the one hand, the COD removal obtained with the UD-FPR configuration shows percentage values higher than TOC removal which implies a higher generation of oxidised compounds after the process.
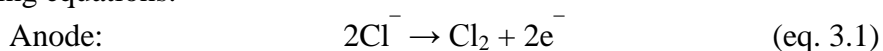
Table 1. TOC and COD removal percentages obtained using U-FPR and UD-FPR configurations for the electrolysis of a synthetic dye solution of 1.0 g L^{-1} C.I. Reactive Black 5. Electrolyte: 0.1 M Na$_2$SO$_4$ or 0.1 M NaCl. Processes performed at (a) 125 mA cm^{-2} and (b) 50 mA cm^{-2}. Electrode area = 48 cm^2; V$_{sol}$ = 0.45 L; Q$_F$ = 240 Ah L^{-1}.

(a) Electrolyte	Configuration	ΔCOD (%)	ΔTOC (%)
	UD-FPR	62.35	49.09
Na$_2$SO$_4$	D-FPR	50.99	60.51
	UD-FPR	92.26	38.15
NaCl	D-FPR	97.52	69.44
(b) Electrolyte	Configuration	ΔCOD (%)	ΔTOC (%)
	UD-FPR	64.18	44.80
Na$_2$SO$_4$	D-FPR	59.51	77.80
	UD-FPR	91.32	47.07
NaCl	D-FPR	95.95	61.34

On the contrary, the electrochemical treatment carried out with the D-FPR configuration of the filter press reactor showed variable results depending on the type of electrolyte employed. When 0.1 M NaCl was employed, the same behaviour as that observed with the UD-FPR configuration was observed, that is, COD removals were higher than the mineralisation obtained. When 0.1 M Na$_2$SO$_4$ was selected as electrolyte, the observed behaviour was the opposite: TOC removals were higher than COD removals. Therefore, it seems that the use of sulphate implies a greater mineralisation rate than the use of chloride.
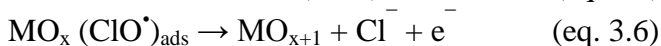
With regard to the applied current density, results from Table 1 prove that the degradation of the dye does not really depend on the current density. As it can be seen, only when the UD-FPR configuration was used at 50 mA cm^{-2} in the presence of 0.1 M Na$_2$SO$_4$, is the oxidation and mineralisation degree higher than the process at 125 mA cm^{-2} with the same configuration of the reactor, although the difference is not very noteworthy. The rest of the electrochemical processes, with both D-FPR and UD-FPR configurations, and regardless of whether an electrolyte was used, gave similar TOC and COD removals.

On the other hand, it was found that, for D-FPR and UD-FPR configurations where 0.1 M NaCl was selected as electrolyte, the COD removal was always higher than the COD removal obtained when the electrolyte was 0.1 M Na$_2$SO$_4$. This result was found at the two applied current densities, 125 and 50 mA cm^{-2}. This fact is due to the electrogenerated hypochlorite ions (ClO$^-$) according to the following equations:

Anode: $\qquad\qquad\qquad 2Cl^- \rightarrow Cl_2 + 2e^-$ $\qquad\qquad$ (eq. 3.1)

Bulk solution: $Cl_2 + H_2O \rightarrow HOCl + H^+ + Cl^-$ (eq. 3.2)

$HOCl \rightleftarrows H^+ + OCl^-$ (eq. 3.3)

The presence of ClO^- ions produces an indirect oxidation of organic matter [37, 38], apart from the indirect oxidation produced by $OH^\bullet$ radicals and the direct oxidation produced as a consequence of the presence of overoxidised sites (MO_{x+1}), according to the equations 3.4 – 3.7 [39-41].

$MO_x (OH)_{ads} + Cl^- \rightarrow MO_x (ClO^\bullet)_{ads}$ (eq. 3.4)

$MO_x + HClO \rightarrow MO_x (ClO^\bullet)_{ads} + H^+ + e^-$ (eq. 3.5)

$MO_x (ClO^\bullet)_{ads} \rightarrow MO_{x+1} + Cl^- + e^-$ (eq. 3.6)

$MO_x (ClO^\bullet)_{ads} + Cl^- \rightarrow MO_{x+1} + Cl_2 + e^-$ (eq. 3.7)

Moreover, after the electrochemical process performed with an UD-FPR configuration, TOC removal was always practically equal to or less than 50 %, while after the electrochemical process performed with a D-FPR configuration TOC removal were between 60 – 80 %. Therefore, it can be said that the D-FPR configuration is the most appropriate configuration to degrade the organic matter. Once again, the applied current density has not a significant effect in terms of TOC removal.

From a general point of view, TOC removals obtained in the presence of 0.1 M NaCl are equal to or less than TOC removals when 0.1 M Na_2SO_4 was selected as electrolyte. The standard potentials of Cl_2/Cl^- and $HClO/Cl_2$ are +1.36 V and +1.63 V, respectively, and the standard potential of $OH^\bullet$, H^+/H_2O is +2.70 V [42]. Taking into account all the results presented above, the presence of the "active chlorine" does not contribute to the mineralisation process, but it increases the oxidation rate of the solution. Therefore, the mineralisation process is basically due to the $OH^\bullet$ radicals which constitute the main oxidant when sulphate is used as electrolyte. This behaviour has been observed by several authors [43, 44]. In the case of Song et al., they studied the oxidation of the bifunctional dye C.I. Reactive Red 195 in the presence and in the absence of chloride, confirming the same behaviour by GC-MS analyses [44].

3.2. Average Oxidation State (AOS) and Carbon Oxidation State (COS)

Changes of the mean oxidation state of the organic carbon during the electrochemical treatments were also determined. The average oxidation state (AOS) of the organic carbon can be calculated by means of the ratio between COD and TOC values as follows [45-48]:

$$AOS = \frac{4 \cdot (TOC - COD)}{TOC}$$ (eq. 3.8)

where *COD* and *TOC* (expressed as mol L^{-1}) were determined at the sampling time. Thus, the AOS parameter is only referred to the organic matter remaining in the solution. Nevertheless, though

AOS is not an indicator of the efficiency of the electrochemical process, it indicates variations in the composition of dissolved organic matter after the process.

Figure 3 shows the evolution of AOS observed during the electrochemical processes carried out with the two different configurations of the filter press reactor. All these processes were performed at 125 mA cm^{-2} in the presence of either 0.1 M Na$_2$SO$_4$ or 0.1 M NaCl as electrolyte. When the electrochemical process was done with an UD-FPR configuration and 0.1 M Na$_2$SO$_4$ was selected as electrolyte (Fig.3–a), four different stages can be distinguished. In the first stage, AOS increased up to 20 Ah L^{-1} of applied specific charge. This increase implies that the organic compounds are being continuously oxidised but not completely mineralised. In other words, structural changes are taking place in the solution at those charge values. Following this, AOS showed a negative trend so those intermediates generated in the previous stage are now being degraded. From 25 Ah L^{-1} onwards, a new increase in AOS values was observed due to a new partial oxidation. Finally, the last stage showed a stabilization of AOS which means that the oxidation and the mineralisation rates are comparable.
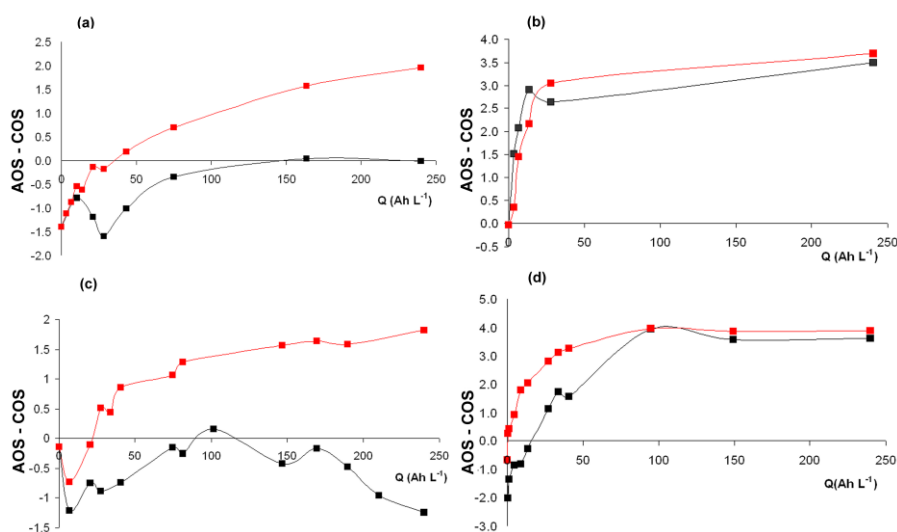

Figure 3. AOS (■) and COS (■) evolutions obtained for different configurations of the filter press reactor in the presence of either 0.1 M Na$_2$SO$_4$ or 0.1 M NaCl: (a) UD-FPR configuration and 0.1 M Na$_2$SO$_4$ as electrolyte; (b) UD-FPR configuration and 0.1 M NaCl as electrolyte; (c) D-FPR configuration and 0.1 M Na$_2$SO$_4$ as electrolyte; (d) D-FPR configuration and 0.1 M NaCl as electrolyte. Current density in all cases: 125 mA cm^{-2}.

Fig.3–b shows the AOS evolutions with an UD-FPR configuration in the presence of NaCl. Three different stages can be distinguished. First of all, AOS increased sharply so the organic matter was being strongly oxidised. Later, the AOS trend showed a slight decrease which means a greater mineralisation of intermediates. Finally, AOS shows a moderate increase. Fig.3–c corresponds to the D-FPR configuration in the presence of 0.1 M Na$_2$SO$_4$ as electrolyte. In this case, after a brief sharp decrease, two different stages can be distinguished. In the first one, AOS increased until 100 Ah L^{-1} approximately and, later, AOS decreased to more negative values. These two trends mean that, at the beginning of the process, the organic compounds were oxidised up to 100 Ah L^{-1}. All the oxidised

intermediates that appeared in the first stage were later mineralised (second stage). The AOS values when the D-FPR configuration was employed with 0.1 M NaCl as electrolyte also showed two stages (Fig. 3–d). While in the first stage a similar trend to the case of the D-FPR configuration using 0.1 M Na_2SO_4 was observed, the second stage showed a stable and invariable trend of AOS which denotes similar oxidation and mineralisation rates.

The oxidation degree evolution can be completed by the estimation of the carbon organic state (COS) associated with the process. COS was calculated by means of the following expression [49]:

$$COS = \frac{4 \cdot (TOC_0 - COD)}{TOC_0} \quad \text{(eq. 3.9)}$$

where TOC_0 is the initial total organic carbon of the solution and COD was determined at the sampling time (both parameters expressed as mol L^{-1}). Note that in this formula, carbon eliminated from the solution in the form of CO_2 (whose oxidation state is +4) is also considered in the calculation so this parameter represents the carbon oxidation efficiency. The evolution of COS is also represented in Fig. 3–a, 3-b, 3-c and 3-d. In all cases, an increasing trend of this parameter was observed. The much higher slope suggests that the carbon oxidation is more efficient (Fig. 3–b and 3-d). Moreover, results show that the maximum value of COS (+4, corresponding to CO_2) was practically obtained when NaCl was employed with both D-FPR and UD-FPR configurations (Fig.3–b and 3-d). Therefore, it seems that the presence of chloride enhances to a great extent the processes occurring in both configurations. Nevertheless, when Na_2SO_4 was employed, the maximum value of COS obtained for these processes was about 2.0, almost half the degree of oxidation obtained in the presence on chloride. Actually, this fact is in accordance with the results of COD removals for these processes (Table 1). While the COD removal obtained in the presence of NaCl is about 90 – 100 %, the results of COD removals obtained with Na_2SO_4 are between 50 – 60 %.

3.3. Average Current Efficiency (ACE)

The average current efficiencies (ACE) for the electrochemical processes performed with both D-FPR and UD-FPR configurations under given experimental conditions can be calculated considering the values of COD [41, 50-53] by the following equation:

$$ACE = \frac{COD_0 - COD_t}{8 \cdot I \cdot t} \cdot F \cdot V \cdot 100 \quad \text{(eq. 3.10)}$$

where COD_0 and COD_t are the initial COD and the COD after 240 Ah L^{-1} (g O_2 L^{-1}) respectively, F is the Faraday constant (96487 C mol^{-1}), V is the volume of the synthetic wastewater (L), I is the applied current (A), t is the time of electrolysis (s) and 8 is the equivalent weight of oxygen. Table 2 shows ACE (%) values obtained by this method as a function of the configuration of the filter press reactor, the current density and the electrolyte nature. In the case of using 0.1 M Na_2SO_4

as electrolyte (Table 2-a), results show that ACE calculated at the point of complete decolourisation ($Q_{1\% \, AZO}$) was between 2.0 and 3.0 in all cases except when using the D-FPR configuration at 125 mA cm^{-2}. From a general point of view, the ACE values at this point of the electrolysis are always higher than at the end (Q_F). This can be explained in terms of the degradation reaction of both the dye and the intermediates generated during the electrolysis, since this reaction is the main reaction at the beginning of the electrolysis. However, as the concentration of these compounds diminishes, the electrolysis of water is more noticeable and this leads to lower ACE values. Moreover, for the two configurations, when the current density increases a reduction of the ACE values at the moment of complete decolourisation was observed. This behaviour occurs because the higher the current density is, the greater the extent of the oxygen evolution reaction. On the basis on these results, it can be said that the degradation of C.I. Reactive Black 5 is controlled by mass transport. This means that the degradation rate is limited by the mass transfer from the bulk solution to the electrode surface [54-56].
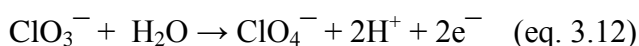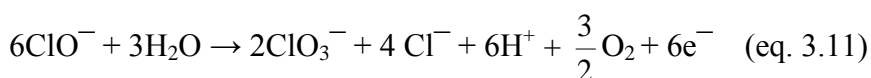
As in the case of 0.1 M Na$_2$SO$_4$, when using 0.1 M NaCl as electrolyte ACE values at the moment of complete decolourisation ($Q_{1\% \, AZO}$) were always higher than at the end of the electrolysis (Q_F), as can be observed in Table 2-b.

Table 2. ACE values obtained for the electrochemical treatment using UD-FPR and D-FPR configurations of the filter press reactor in the presence of (a) 0.1 M Na$_2$SO$_4$ as electrolyte; (b) 0.1 M NaCl as electrolyte. The ACE values were calculated at the moment of complete decolourisation ($Q_{1\%AZO}$) and at the end of the electrolysis (Q_F) at 125 mA cm^{-2} and 50 mA cm^{-2} current densities. Synthetic dye solutions of 1.0 g L^{-1} C.I. Reactive Black 5. Total applied specific charge: 240 Ah L^{-1}. Electrode area = 48 cm^2; V_{sol} = 0.45 L.

| (a) j (mA cm^{-2})	Configuration	$Q_{1\%AZO}$ (Ah L^{-1})	Q_F (Ah L^{-1})
	UD-FPR	2.37	0.62
125	D-FPR	0.64	0.44
	UD-FPR	2.57	0.63
50	D-FPR	2.72	0.48
(b) j (mA cm^{-2})	Configuration	$Q_{1\%AZO}$ (Ah L^{-1})	Q_F (Ah L^{-1})
	UD-FPR	12.16	0.97
125	D-FPR	32.71	0.88
	UD-FPR	10.19	1.05
50	D-FPR	15.11	0.15

On the other hand, it was observed that, at the moment of complete decolourisation, the higher the current density was, the higher the ACE values were. On account of this fact, it can be concluded that the degradation mechanism in the presence of 0.1 M NaCl was controlled by charge transfer. In other words, a higher polarisation of the electrode surface produces a greater concentration of "active chlorine" which finally results in a greater degradation of the dye and intermediates. As can be seen, for the processes carried out with the D-FPR configuration, the values obtained at complete decolourisation were always higher than those obtained, also at complete decolourisation, when the UD-FPR configuration was used. In fact, at 125 mA cm^{-2} the use of one or another configuration of the filter press reactor showed significant differences in the ACE values. This can be explained by

considering the pH changes that occurred in solution during the electrochemical process carried out with each one of the configurations. Although the initial dye solution presented a strong alkaline pH, when the D-FPR configuration was used, the pH diminished drastically due to the hydroxyl groups' consumption. In contrast, the pH of the solution during and after the electrochemical process performed with the UD-FPR configuration was neutral or slightly alkaline. According to equation 3.3, during the process done with D-FPR configuration (acidic pH) "active chlorine" is present in the form of hypochlorous acid which has higher oxidation potential (1.49 V) than that of hypochlorite (0.89 V), the latter being prevalent in solutions resulting from using the UD-FPR configuration (where the pH is slightly alkaline). Moreover, in alkaline solutions, the lower degradation efficiency is also due to the formation of chlorate or perchlorate according to the following equations [57-62]:

$$6ClO^- + 3H_2O \rightarrow 2ClO_3^- + 4\,Cl^- + 6H^+ + \frac{3}{2}O_2 + 6e^- \quad \text{(eq. 3.11)}$$

$$ClO_3^- + H_2O \rightarrow ClO_4^- + 2H^+ + 2e^- \quad \text{(eq. 3.12)}$$

Other loss reactions can also occur in the bulk solution [58, 60]. These are

$$ClO^- \rightarrow O_2 + 2Cl^- \quad \text{(eq. 3.13)}$$

$$2HClO + ClO^- \rightarrow ClO_3^- + 2Cl^- + 2H^+ \quad \text{(eq. 3.14)}$$
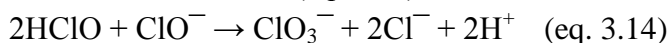
Moreover, other possible reactions can take place at the cathode simultaneously with the reaction of hydrogen evolution [58, 60]:

$$ClO^- + H_2O + 2e^- \rightarrow Cl^- + 2OH^- \quad \text{(eq. 3.15)}$$

The occurrence of the loss reactions given by eq. 3.12, 3.13 and 3.14 is very probable when the reactor is undivided (UD-FPR). This, together with the lower oxidation potential of hypochlorite ions, could further slow the rate of dye destruction under alkaline conditions.

3.4. Decolourisation kinetics

Decolourisation during the electrolysis was also monitored by means of the HPLC technique and spectrophotometry. The HPLC technique was employed to evaluate the evolution of the dye concentration as the applied specific charge increased. The spectrophometry technique was also employed to confirm the decolourisation obtained. This decolourisation followed pseudo-first order kinetics in all cases. UV-Visible spectra of C.I. Reactive Black 5 during the electrolysis performed with both configurations and in the presence of 0.1 M Na_2SO_4 are shown in Figure 4.

The spectra showed maximum absorption in the range of visible light at a wavelength of 600 nm. During the electrolysis a complete disappearance of this band was observed in all cases, which means a complete solution decolourisation. This decolourisation can be also observed in the inset photographs. The appearance of bands in the UV region of the spectrum indicates the presence of

conjugated double bonds in the molecular structure [63, 64]. The transitions $\Pi \rightarrow \Pi^*$ are responsible for the absorbance of the dye molecule in the UV region.
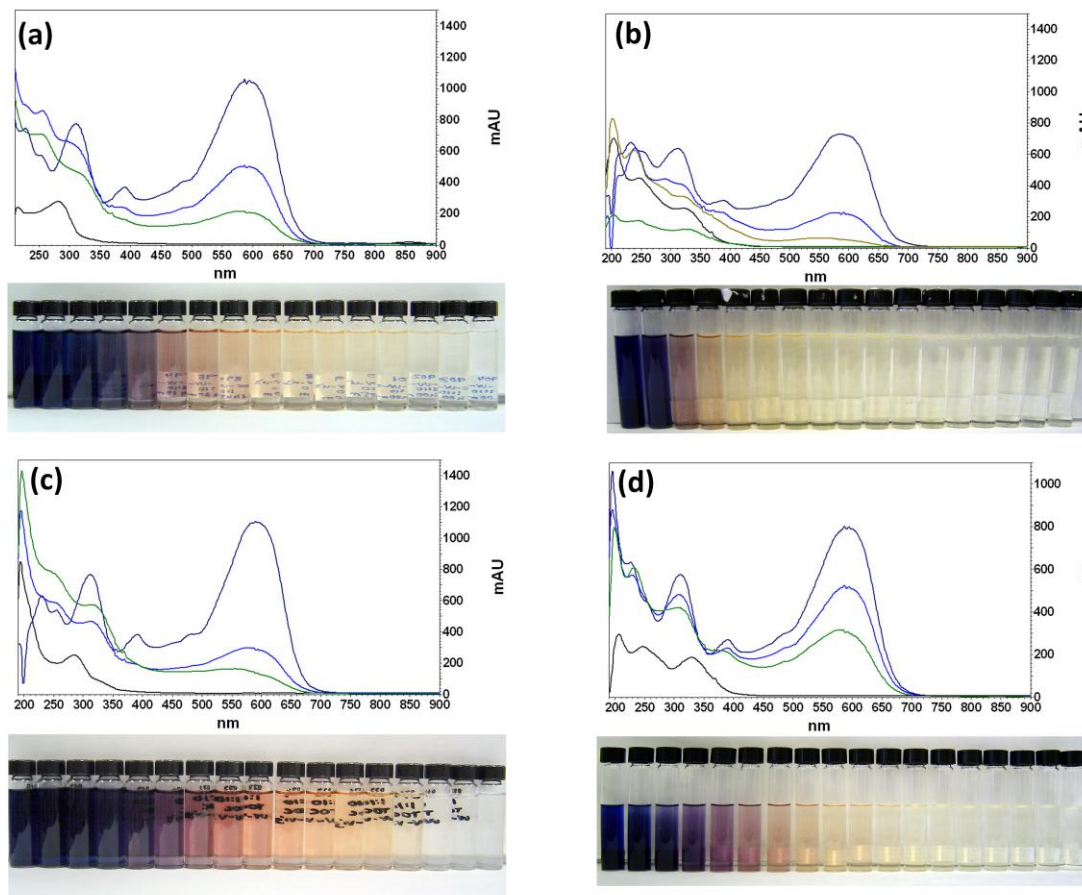

Figure 4. UV-Visible spectra evolution until complete decolourisation and images of the decolourisation progress for all the processes studied: (a) with an UD-FPR configuration and 125 mA cm^{-2} current density; (b) with a D-FPR configuration and 125 mA cm^{-2} current density; (c) with an UD-FPR configuration and 50 mA cm^{-2} current density; (d) with a D-FPR configuration and 50 mA cm^{-2} current density. Synthetic dye solutions of 1.0 g L^{-1} C.I. Reactive Black 5. Electrolyte: 0.1 M Na$_2$SO$_4$ in all cases; Electrode area = 48 cm^2; V_{sol} = 0.45 L.

The intensity and shift of the UV bands along the electrolysis time provides valuable information about the content of aromatic compounds in solution. Since the intensity of these bands did not entirely diminish, it seems that aromatic compounds are being degraded to some extent during the electrolysis. Actually, this in accordance with TOC removal percentages (from 45 to 75 %, see Table 1) since the organic matter remaining in solution after treatment corresponds to the non-destroyed aromatic compounds. Table 3 includes the kinetic results as well as the charge values to obtain a complete decolourisation with both configurations, both current densities and both electrolytes. All these results are showed in a decreasing order of the decolourisation rates. From the kinetic results presented in Table 3-a, it can be seen that, in the presence of 0.1 M Na$_2$SO$_4$ as electrolyte, the processes carried out at 50 mA cm^{-2} presented higher decolourisation rates. This trend

occurs because, under these conditions, an increase in current density implies that the oxygen reaction becomes more noticeable.

Table 3. Decolourisation rate constants and charge values for a complete decolourisation using UD-FPR and D-FPR configurations with: (a) 0.1 M Na_2SO_4 as electrolyte; (b) 0.1 M NaCl as electrolyte. Synthetic dye solutions of 1.0 g L^{-1} C.I. Reactive Black 5. Electrode area = 48 cm^2; V_{sol} = 0.45 L. [a]Q = 0 – 0.70 Ah L^{-1}; [b]Q = 0.70 – 1.13 Ah L^{-1}.

	Configuration	j (mA cm^{-2})	K_{app} (L $A^{-1}h^{-1}$)	$Q_{1\%AZO}$ (Ah L^{-1})
(a)	UD-FPR	50	0.371	12.88
	D-FPR	50	0.319	14.92
Na_2SO_4	UD-FPR	125	0.239	20.30
	D-FPR	125	0.233	19.76
(b)	D-FPR	50	1.267^a 4.932^b	1.46
NaCl	D-FPR	125	2.021	2.38
	UD-FPR	125	0.990	4.89
	UD-FPR	50	0.594	8.23

Figure 5 compares the different UV-Visible evolutions obtained in the presence of 0.1 M NaCl as electrolyte. It is clear that the addition of NaCl to the dye solution is a key factor since the presence of chloride can enhance the degradation efficiency and shortens the applied specific charge needed to decolourise. As the evolution of UV-Visible spectra revealed, the band at 600 nm disappeared completely in all cases which means a complete decolourisation of the initial solution. Once again, the bands observed in the UV region presented an important diminution so the aromatic compounds present in solution were also partially degraded. Apart from this, in the light of the information given in section 3.3, the type of process carried out is of great importance when NaCl is used as electrolyte. As shown in Table 3-b, when the D-FPR configuration was employed the processes presented the best kinetic rates and this can be explained in terms of pH. Solutions during and after the electrochemical processes done in a D-FPR configuration presented an acidic pH which favours the presence of hypochlorous acid as "active chlorine" whose standard potential is much higher than that for hypochlorite (which is present when the UD-FPR configuration was used). It should be also noted that the process performed with a D-FPR configuration at 50 mA cm^{-2} presented a double kinetic trend which could be related to mechanism changes during the decolourisation process. Moreover, the ACE value at complete decolourisation for this process was 15.11 (against an ACE value of 32.71 for D-FPR configuration at 125 mA cm^{-2}).
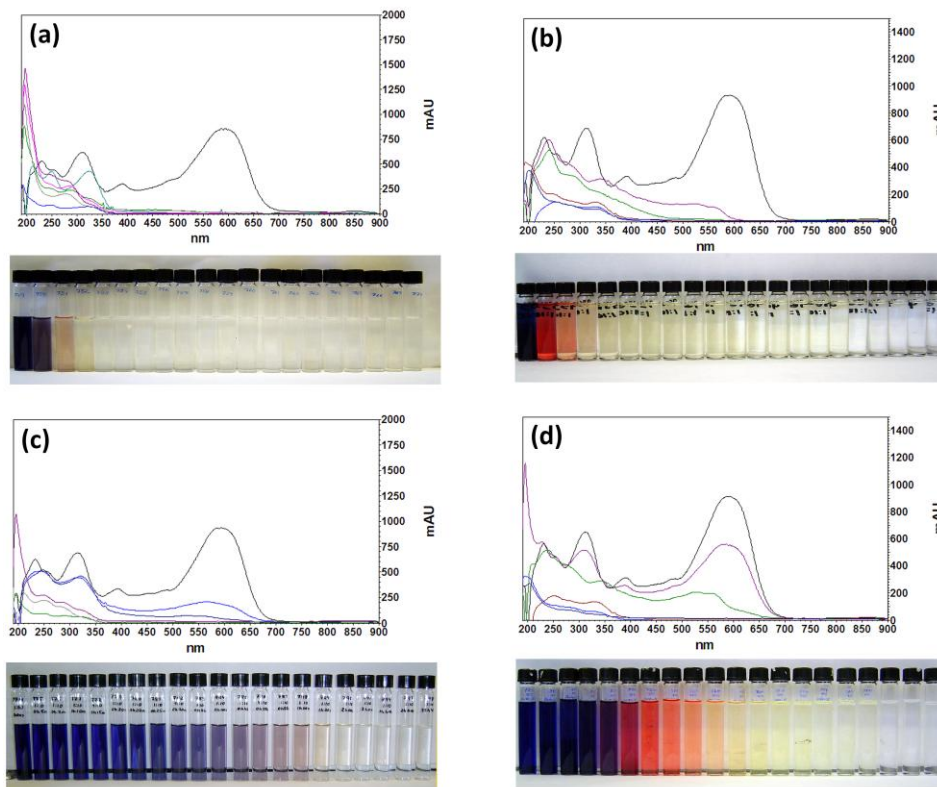
Figure 5. UV-Visible spectra evolution until complete decolourisation and images of the decolourisation progress for all the processes studied: (a) with an UD-FPR configuration and 125 mA cm^{-2} current density; (b) with a D-FPR configuration and 125 mA cm^{-2} current density; (c) with an UD-FPR configuration and 50 mA cm^{-2} current density; (d) with a D-FPR configuration and 50 mA cm^{-2} current density. Synthetic dye solutions of 1.0 g L^{-1} C.I. Reactive Black 5. Electrolyte: 0.1 M NaCl in all cases; Electrode area = 48 cm^2; V$_{sol}$ = 0.45 L.

In literature, it is reported that the azo bond breakage is the initial step of dye degradation which leads to decoloured intermediates in the bulk solution [65]. Once the chromophore group has been broken, the rest of the dye molecule and/or intermediates are degraded. Assuming that the degradation process is controlled by charge transfer in the presence of chloride, it seems clear that at the lower current density the degradation efficiency presented lower ACE values than at 125 mA cm^{-2}.

3.5. HPLC analyses

Detection at the maximum absorption wavelength was used to follow the dependence of the dye concentration diminution over time. Therefore, the evolution of the dye concentration can be monitored by using a 600 nm wavelength detector. The information obtained has been summarized in Figure 6 for both electrolytes employed in this work and both current densities considered.
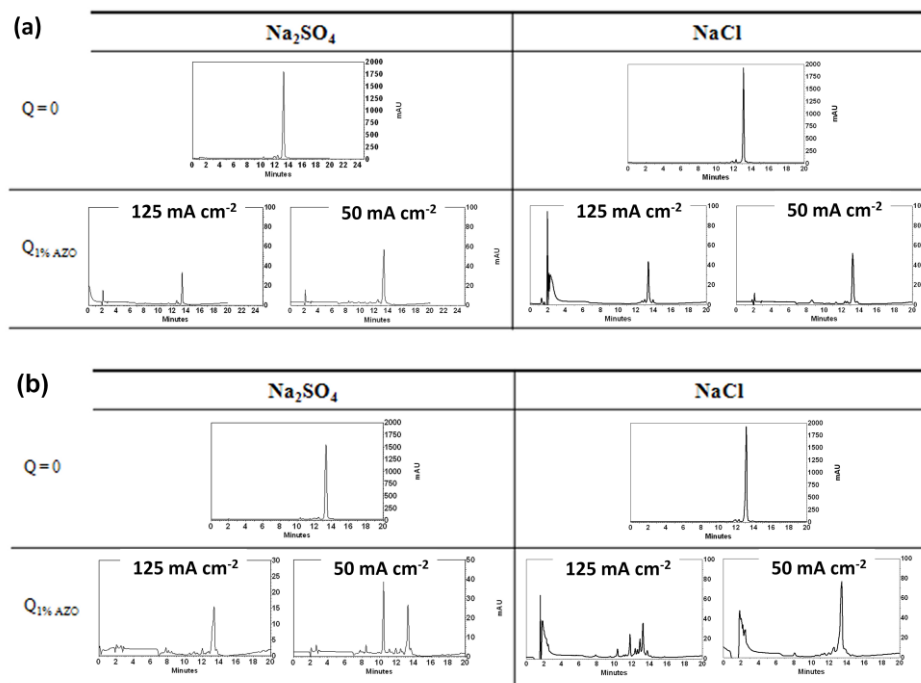
Figure 6. Chromatographic analyses of the initial samples (before the electrochemical processes, Q =0) and samples collected at the moment of complete decolourisation ($Q_{1\%AZO}$). Current density indicated at the top of each chromatogram. (a) Electrochemical processes carried out with an UD-FPR configuration; (b) Electrochemical processes carried out with a D-FPR configuration. Detection wavelength: 600 nm. Synthetic dye solutions of 1.0 g L^{-1} C.I. Reactive Black 5. Electrolyte concentration: 0.1 M Na_2SO_4 and 0.1 M NaCl. Electrode area = 48 cm^2. V_{sol} = 0.45 L.

The chromatographic results obtained when the UD-FPR configuration was used are showed in Fig. 6-a. Moreover, the chromatographic results obtained with the D-FPR configuration are showed in Fig. 6-b. In all cases, the initial solution (Q =0) as well as chromatograms obtained at complete decolourisation ($Q_{1\%AZO}$) are included. Chromatograms corresponding to un-treated solutions showed a main peak at about 14 minutes. At the moment of complete decolourisation a marked diminution of the dye peak was observed in all cases, which clearly indicates that the majority of the azo group present in solution was degraded.

Figure 7 shows representative chromatograms of initial, intermediate (at complete decolourisation) and final solutions of C.I. Reactive Black 5 when the detector wavelength was set at 250 nm. The chromatographic information obtained at this wavelength is related to the presence of aromatic compounds resulting from the electrochemical treatment of the dye solution. The chromatograms for the un-treated solution showed a main peak at t_R about 14 minutes. Considering the aromatic nature of the dye, it is clear that this peak corresponds to the dye before the electrochemical treatment. At the moment of complete decolourisation ($Q_{1\% AZO}$) it was found that, independently of the electrolyte employed, this chromatographic peak completely disappeared. As a result, a set of new chromatographic peaks appeared. In the case of using the UD-FPR configuration, a main chromatographic peak was detected at t_R = 2 minutes which was also observed in chromatograms corresponding to final solutions (Q = 240 Ah L^{-1}), as shown in Fig. 7-a. This suggests that, after an

initial breakage of the dye, a main intermediate whose stability in solution was considerable was generated.
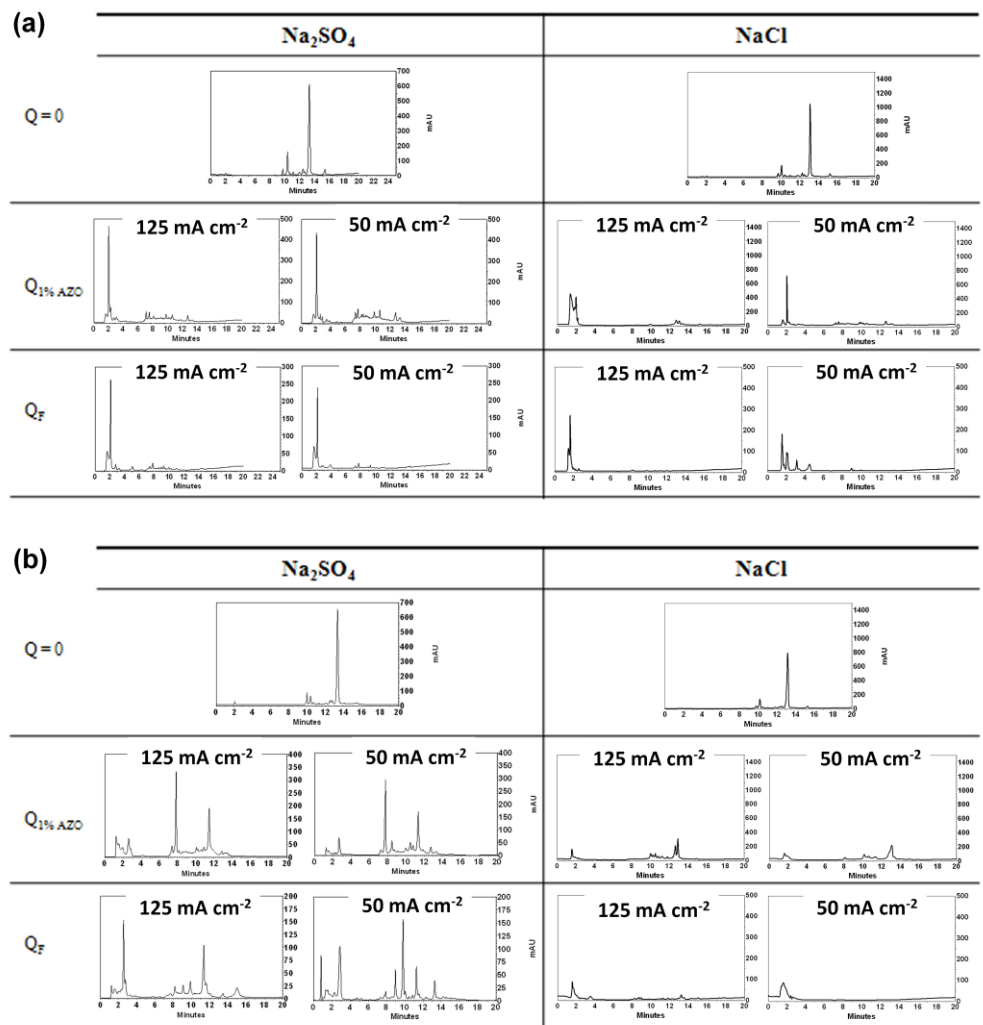

Figure 7. Chromatographic analyses of the initial samples (before the electrochemical processes, Q =0), samples collected at the moment of complete decolourisation ($Q_{1\% AZO}$) and final samples (Q = 240 Ah L^{-1}). Current density indicated at the top of each chromatogram. (a) Electrochemical processes carried out with an UD-FPR configuration; (b) Electrochemical processes carried out with a D-FPR configuration. Detection wavelength: 250 nm. Synthetic dye solutions of 1.0 g L^{-1} C.I. Reactive Black 5. Electrolyte concentration: 0.1 M Na_2SO_4 and 0.1 M NaCl. Electrode area = 48 cm^2. V_{sol} = 0.45 L.

In contrast, chromatographic analyses of the dye solution during and after the electrochemical process done with the D-FPR configuration in the presence of 0.1 M Na_2SO_4 revealed the appearance of a greater number of peaks (Fig. 7-b). This indicates that, when the electrochemical process was performed with the D-FPR configuration, the degradation mechanism is clearly different from that corresponding to the use of the UD-FPR configuration. In addition to this, the complete disappearance of some of these peaks during the process done with the D-FPR configuration and the subsequent

appearance of other peaks is clear evidence of the successive degradation of some early intermediates which then generate other secondary compounds. This last behaviour was observed for both electrolytes employed.

4. CONCLUSIONS

In the present work, the electrochemical treatment for the degradation of C.I. Reactive Black 5 using Ti/SnO$_2$-Sb-Pt as anode and stainless steel as cathode has been evaluated. It has been demonstrated that solutions containing this dye can be degraded to a great extent by using either UD-FPR or D-FPR configurations. Although the electrochemical processes using the UD-FPR configuration generated some intermediates, these compounds showed a highly oxidised state. On the other hand, the relative TOC and COD removals after the electrochemical process carried out with the D-FPR configuration were influenced by the type of electrolyte employed. Thus, the addition of chloride enhanced the oxidation and the decolourisation processes. In fact, complete COD removal was achieved in the presence of chloride. With regard to the mineralisation in the presence of chloride, from a general point of view it can be said that it is equal to or less than the mineralisation obtained when sulphate was used (with the exception of the oxidation at 125 mA cm^{-2}). These results were also confirmed by AOS and COS analyses. Moreover, regardless of whether chloride or sulphate was employed as electrolyte, a complete colour disappearance was obtained in all cases showing pseudo-first order kinetics. The current density did not have any considerable influence on TOC and COD removal. On the contrary, the efficiency was significantly affected by current density as well as the type of electrolyte and the configuration considered. Then, the optimum operational conditions to obtain the best efficiency corresponded to the use of chloride using the D-FPR configuration at 125 mA cm^{-2}. Under these conditions, the process was shown to be charge transfer controlled. HPLC analyses revealed differences among all the electrochemical processes which implies different degradation mechanisms. Since the real limitation of the use of chloride as electrolyte is the formation of chlorinated compounds, further research is currently in progress to verify the presence and concentration of these compounds in solutions after electrochemical treatment.

References

1. E. Forgacs, S.F. Cserhati and G. Oros, *Environ. Int*, 30 (2004) 953.
2. C.A. Martínez-Huitle and E. Brillas, 2009. *Appl. Catal. B*, 87 (2009) 105.
3. Y. Anjaneyulu, N. Sreedhara Chary and S. Suman Raj, *Environ. Sci. Biotechnol*, 4 (2005) 245.

4. M.C. Venceslau, S. Tom and J.J. Simon, *Environ.Technol*, 15 (1994) 917.
5. S.J. Perey, L. Brian, C. Pei, H. Chin-Pao and C.K. Daniel, *Water Environ. Res*, 78 (2006) 26.
6. T. Robinson, G. McMullan, R. Marchant and P. Nigam, *Bioresource Technol*, 77 (2001) 247.
7. R.L.M. Allen, *Colour Chemistry*, Nelson & Sons, London (1971).
8. R.M. Christie, *Colour Chemistry*, The RSC Paperbacks, UK (2001)
9. K. Sarayu, K. Swaminathan and S. Sandhya, *Dyes Pigments*, 75 (2007) 362.
10. M. Neamtu, A. Yediler, I. Siminiceanu and A. Kettrup, *J. Photoch. Photobio*, A, 161 (2003) 87.
11. M.S. Lucas, A.A. Dias, A. Sampaio, C. Amaral and J.A. Peres, *Water Res*, 41 (2007) 1103.
12. P. Peralta-Zamora, A. Kunz, S. Gomes de Moraes, R. Pelegrini, P. de Campos Moleiro, J. Reyes and N. Durán, *Chemosphere*, 38 (1999) 835.
13. K. Swaminathan, S. Sandhya, S.A. Carmalin, K. Pachhade and Y.V. Subrahmanyam, *Chemosphere*, 50 (2003) 619.
14. L. Núñez, J.A. García-Hortal and F. Torrades, *Dyes Pigments*, 75 (2007) 647.
15. M.M. Dávila-Jiménez, M.P. Elizalde-González and A.A. Peláez-Cid, *Colloid Surf. A*, 254 (2005) 107.
16. O.T. Can, M. Bayramoglu and M. Kobya, *Ind. Eng. Chem. Res*, 42 (2003) 3391.
17. M. Cerón-Rivera, M.M. Dávila-Jiménez and M.P. Elizalde-González, *Chemosphere*, 55 (2004) 1.
18. N. Daneshvar, H.A. Sorkhabi and M.B. Kasiri, *J.Hazard. Mater*, 112 (2004) 55.
19. A. Faouzi, B. Nasr and G. Abdellatif, *Dyes Pigments*, 73 (2007) 86.
20. A. Fernandes, A. Morão, M. Magrinho, A. Lopes and I. Gonçalves, *Dyes Pigments*, 61 (2004) 287.
21. J. Hastie, D. Bejan, M. Teutli-León and N.J. Bunce, *Ind. Eng. Chem. Res*, 46 (2006) 4898.
22. M. Muthukumar, M.T. Karuppiah and G.B. Raju, *Sep. Purif. Technol*, 55 (2007) 198.
23. P.A. Carneiro, C.S. Fugivara, R.F.P. Nogueira, N. Boralle and M.V.B. Zanoni, Port. *Electrochim. Acta*, 21 (2003) 49.
24. L. Fan, Y. Zhou, W.Yang, G. Chen and F. Yang, *J. Hazard. Mater*, 137 (2006)1182.
25. L. Fan, Y. Zhou, W.Yang, G. Chen and F. Yang, *Dyes Pigments*, 76 (2008) 440.
26. M.C. Gutierrez, M. Pepió and M. Crespi, *Color. Technol*, 118 (2002) 1.
27. M. Panizza, C. Bocca and G. Cerisola, *Water Res*, 34 (2000) 2601.
28. F. Yi, S. Chen and C. Yuan, *J. Hazard. Mater*, 157 (2008) 79.
29. L.S. Andrade, T.T. Tasso, D.L. da Silva, R.C. Rocha-Filho, N. Bocchi and S.R. Biaggio, *Electrochim. Acta*, 54 (2009) 2024.
30. E.J. Weber and V.C. Stickney, *Water Res*, 27 (1993) 63.
31. C. O'Neill, F.R. Hawkes, D.L. Hawkes, N.D. Lourenço, H.M. Pinheiro and W. Deleé, *J. Chem. Technol. Biot*, 74 (1999) 1009.
32. A.I. del Río, J. Fernández, J. Molina, J. Bonastre and F. Cases, *Desalination*, 273 (2011) 428.
33. F. Vicent, E. Morallón, C. Quijada, J.L. Vázquez, A. Aldaz and F. Cases, 1998. *J. Appl. Electrochem*. 28 (1998) 607.
34. F. Montilla, E. Morallón, A. De Battisti,, S. Barison, S. Daolio and J.L. Vázquez, *J. Phys. Chem. B*, 108 (2004) 15976.
35. F. Montilla, E. Morallón, A. De Battisti, A. Benedetti, H. Yamashita and J.L. Vázquez, *J. Phys. Chem. B*, 108 (2004) 5044.
36. F. Montilla, E. Morallón, A. De Battisti and J.L. Vázquez, *J. Phys. Chem. B*, 108 (2004) 5036.
37. Ch. Comninellis, *Electrochim. Acta*, 39 (1994) 1857.
38. Ch. Comninellis and A. Nerini, *J. Appl. Electrochem*, 25 (1995) 23.
39. N. Mohan and N. Balasubramanian, *J. Hazard. Mater. B*, 136 (2006) 239.
40. N. Mohan, N. Balasubramanian and C.A. Basha, *J. Hazard. Mater,* 147 (2007) 644.
41. D. Rajkumar, J.G. Kim and K. Palanivelu, *Chem. Eng. Technol*, 28 (2005) 98.
42. U. Schümann and P. Gründler, *Water Res*, 32 (1998) 2835.
43. D. Rajkumar, B. Joo Song and J. Guk Kim, *Dyes Pigments*, 72 (2007) 1.
44. S. Song, J. Fan, Z. He, L. Zhan, Z. Liu, J. Chen and X. Xu, *Electrochim. Acta*, 55 (2010) 3606.

45. A.M. Amat, A. Arques, F. Galindo, M.A. Miranda, L. Santos-Juanes, R.F. Vercher and R. Vicente, *Appl. Catal. B*, 73 (2007) 220.
46. A.E. Greenberg, T.R. Rhodes and L.S. Clesceri, 1985. *Standard Methods for Examination of Water and Wastewater*, APHA/American Water Works Association/Water Pollution Control Federation. Washington DC (1985).
47. F. Montilla, P.A. Michaud, E. Morallón, J.L. Vázquez and Ch. Comninellis, *Electrochim. Acta*, 47 (2002) 3509.
48. W. Stumm and J.J. Morgan, *Aquatic Chemistry*, John Wiley & Sons. New York , (1981).
49. Ch. Comninellis and C. Pulgarin, *J. Appl. Electrochem*, 21 (1991) 703.
50. L.S. Andrade, L.A.M. Ruotolo, R.C. Rocha-Filho, N. Bocchi, S.R. Biaggio, J. Iniesta, V. García-García and V. Montiel, *J. Hazard. Mater*, 153 (2008) 252.
51. A. Kapalka, G. Fóti and Ch. Comninellis, *Electrochemistry for the Environment*, Springer, New York, (2010).
52. J. Iniesta, P.A. Michaud, M. Panizza, G. Cerisola, A. Aldaz and Ch. Comninellis, *Electrochim. Acta*, 46 (2001) 3573.
53. C. Saez, M. Panizza, M.A. Rodrigo and G. Cerisola, *J. Chem. Technol. Biot*, 82 (2007) 575.
54. C.R. Costa and P. Olivi, *Electrochim. Acta*, 54 (2009) 2046.
55. C.A. Martínez-Huitle and S. Ferro, *Chem. Soc. Rev*, 35 (2006) 1324.
56. M. Panizza and G. Cerisola, *J. Hazard. Mater*, 153 (2008) 83.
57. L.R. Czarnetzki and L.J.J. Janssen, *J. Appl. Electrochem*, 22 (1992) 315.
58. P. Kariyajjanavar, N. Jogttappa and Y. Arthoba Nayaka, *J. Hazard. Mater*, 190 (2011) 952.
59. L. Szpyrkowicz, C. Juzzolino, S.N. Kaul, S. Daniele and M.D. de Faveri, *Ind. Eng. Chem. Res*, 39 (2000) 3241.
60. S. Trasatti, *Electrochim. Acta*, 32 (1987) 369.
61. A.G. Vlyssides, D. Papaioannou, M. Loizidoy, P.K. Karlis and A.A. Zorpas, *Waste Management*, 20 (2000) 569.
62. M. Zhou and J. He, *Electrochim. Acta*, 53 (2007) 1902.
63. R.M. Silverstein, G.C. Bassler and T.C. Morrill, *Spectrometric identification of organic compounds,* John Wiley&Sons, New York, (1974)
64. E. Pretsh, P. Bühlmann, C. Affolter and A. Herrera, R. Martínez, *Determinación structural de compuestos orgánicos*, Springer-Verlag Berlin Heidelberg, New York (2000).
65. M.C. Gutiérrez and M. Crespi, *J. Soc. Dyers Colourists*, 115 (1999) 342.